PASJ: Publ. Astron. Soc. Japan **60**, S25–S33, 2008 February 20

In-Orbit Timing Calibration of the Hard X-Ray Detector on Board Suzaku

Yukikatsu TERADA,[1] Teruaki ENOTO,[2] Ryouhei MIYAWAKI,[2] Yoshitaka ISHISAKI,[3] Tadayasu DOTANI,[4] Ken EBISAWA,[4] Masanobu OZAKI,[4] Yoshihiro UEDA,[5] Lucien KUIPER,[6] Manabu ENDO,[7] Yasushi FUKAZAWA,[8] Tsuneyoshi KAMAE,[9] Madoka KAWAHARADA,[10] Motohide KOKUBUN,[4] Yoshikatsu KURODA,[7] Kazuo MAKISHIMA,[2,10] Kazunori MASUKAWA,[7] Tsunefumi MIZUNO,[8] Toshio MURAKAMI,[11] Kazuhiro NAKAZAWA,[2] Atsushi NAKAJIMA,[7] Masaharu NOMACH,[12] Naoki SHIBAYAMA,[7] Tadayuki TAKAHASHI,[4] Hiromitsu TAKAHASHI,[8] Makoto S. TASHIRO,[1] Toru TAMAGAWA,[10] Shin WATANABE,[4] Makio YAMAGUCHI,[7] Kazutaka YAMAOKA,[13] and Daisuke YONETOKU[11]

[1]*Department of Physics, School of Science, Saitama University, 255 Shimo-Ohkubo, Sakura, Saitama 338-8570*
terada@phys.saitama-u.ac.jp
[2]*Department of Physics, School of Science, The University of Tokyo, 7-3-1 Hongo, Bunkyo-ku, Tokyo 113-0033*
[3]*Department of Physics, Tokyo Metroporitan University, 1-1 Minami-Osawa, Hachioji, Tokyo 192-0397*
[4]*Institute of Space and Astronautical Science, Japan Aerospace Exploration Agency (ISAS/JAXA), 3-1-1 Yoshinodai, Sagamihara, Kanagawa 229-8510*
[5]*Department of Astronomy, Kyoto University, Kitashirakawa-Oiwake-cho, Sakyo-ku, Kyoto 606-8502*
[6]*SRON, National Institute for Space Research, Sorbonnelaan 2, 3584 CA Utrecht, Netherlands*
[7]*Mitsubishi Heavy Industry, Co., Ltd., 1200 Higashi-Tanaka, Komaki, Aichi 485-8561*
[8]*Department of Physical Science, Hiroshima University, 1-3-1 Kagamiyama, Higashi-Hiroshima, Hiroshima 739-8526*
[9]*Stanford Linear Accelerator Center (SLAC), 2575 Sand Hill Road, Menlo Park, CA 94025, USA*
[10]*Makishima Cosmic Radiation Laboratory, RIKEN, 2-1 Hirosawa, Wako, Saitama 351-0198*
[11]*Department of Physics, Faculty of Science, Kanazawa University, Kakuma-machi, Kanazawa, Ishikawa 920-1192*
[12]*Department of Physics, Graduate School of Science, Osaka University, 1-1 Machikaneyama, Toyonaka, Osaka 560-0043*
[13]*Department of Physics and Mathematics, Aoyama Gakuin University, 5-10-1 Fuchinobe, Sagamihara, Kanagawa 229-8558*

(Received 2007 June 16; accepted 2007 August 28)

Abstract

The hard X-ray detector (HXD) aboard the X-ray satellite Suzaku is designed to have a good timing capability with a 61 μs time resolution. In addition to detailed descriptions of the HXD timing system, results of in-orbit timing calibration and the performance of the HXD are summarized. The relative accuracy of time measurements of the HXD event was confirmed to have an accuracy of 1.9×10^{-9} s s^{-1} per day, and the absolute timing was confirmed to be accurate to 360 μs or better. The results were achieved mainly through observations of the Crab pulsar, including simultaneous ones with RXTE, INTEGRAL, and Swift.

Key words: space vehicles: instruments — time — X-rays:general

1. Introduction

The Hard X-ray Detector (HXD: Takahashi et al. 2007; Kokubun et al. 2007) aboard Suzaku (Mitsuda et al. 2007) is a novel cosmic hard X-ray instrument working in the 10–600 keV range. In addition to the very low background level, the wide energy band, and the tightly collimated field of view, yet another important feature of the HXD is its timing capability. This is because time variability, periodic or aperiodic, is an important characteristic of compact cosmic X-ray sources, including neutron stars, white dwarfs, galactic black holes, and active galactic nuclei. Considering the wide range of time scales involved in these variations, we have required the HXD to have a time resolution of 61 μs, and a timing stability on the order of 10^{-9}, typically for one day. To fulfill these goals, we carefully designed the timing system of the HXD, as summarized in section 2, and in more detail in Takahashi et al. (2007) and Kokubun et al. (2007).

The HXD sensor (HXD-S) consists of 16 identical "Well units" working as main detectors (Uchiyama et al. 2001), and 20 surrounding shield counters made of $Bi_4Ge_3O_12$ (BGO) scintillators (Yamaoka et al. 2006). Each Well unit detects incoming X-rays using 2 mm-thick silicon PIN diodes (Sugiho et al. 2001) and Gd_2SiO_5:Ce (GSO) scintillators, both surrounded by a common active BGO shield. The HXD signals from the Well units (called WEL type data) are processed first by an analog electronics package (HXD-AE), and then by digital electronics (HXD-DE).

Before launch, we repeatedly tested and confirmed the HXD timing capability, first at each component level, then incorporating HXD-S, HXD-AE, and HXD-DE (Kokubun et al. 2004; Tashiro et al. 2002; Kawaharada et al. 2004; Terada et al. 2005; Ohno et al. 2005). The tests included confirming time assignments of single WEL-type events with specified time intervals (1, 10, 100, and 1000 s) from a time origin, the detection of periodic signals (with periods of 1, 10, and 100 ms), and measuring the time-interval distribution using random events. After the HXD was mounted on the spacecraft, another series of end-to-end tests incorporating common bus components related to the time assignment (a spacecraft central clock, radio

transmitters, and ground receivers) were repeated.

Through the pre-launch verification, we confirmed that the HXD has the correct timing function, as designed. However, these tests were limited in many aspects. For example, the absolute timing measurements were performed only before the HXD was mounted on the spacecraft. The ground equipment used in these end-to-end tests was not identical to those actually used at the Suzaku tracking center, the Uchinoura Space Center (USC) in southern Japan. Furthermore, once the spacecraft was put into orbit, we had to consider additional complications, such as signal delays due to air propagation to the ground station, and due to cable transmission from the antenna to the signal receivers.

The present paper deals with an in-orbit timing calibration of the HXD. After systematic errors affecting the time assignment are estimated in section 3, we analyze in section 4 highly stable periodic signals from four fast-rotating pulsars, including particularly the Crab pulsar. These tell us the relative accuracy and stability of the time measurements with the HXD. Finally, we verify the absolute timing accuracy of the HXD, by comparing the HXD measurements of the Crab pulsar against those with other X-ray missions and with radio telescopes.

2. The Timing System of the HXD

2.1. Time Assignment of the Suzaku Data

All of the Suzaku data acquired in orbit utilize a common timing system based on a 524288 Hz quartz clock in the spacecraft central data processor (DP). Since the satellite has an orbit with an altitude of 568 km, an eccentricity of < 0.0002, and an inclination of 31°.4, it has an orbital period of about 90 min, making 15 revolutions per day. Therefore, only 5 contacts from the ground station, USC, are available per day. All of the data packets are stored into an on-board data recorder (DR) of 6 Gbits, and transferred via a down link of 4.19 Mbps to ground during satellite contacts. Therefore, the time assignment of the Suzaku data consists of two steps: the first is to calibrate the time origin of the on-board clock against the Universal Time Coordinated (UTC) values during every ground contact; the second is to determine the time when each telemetry packet was edited (usually outside the ground contacts), referring to the on-board clock counts after corrections for their temperature-dependent drifts.

In order to afford the first step of the time assignment, the on-board clock counts, called "TI", are attached to all of the data packets (to be sent to telemetry), which are in the so-called CCSDS (Consultative Committee for Space Data System) format. Each TI has 32 bits, and covers $2^{20}\,\mathrm{s} = 1048576\,\mathrm{s} \simeq 12\,\mathrm{d}$ with $1/4096\,\mathrm{s} = 244\,\mu\mathrm{s}$ being the least significant bit (LSB). When the spacecraft makes ground contacts, these 32-bit values in the TI format are calibrated with ground Rubidium clocks in the UTC format with a stability of $10^{-11}\mathrm{s\ s^{-1}\ month^{-1}}$. That is, all of the relevant information, including the TIs and the temperature of the clock, are gathered every 32 s into special packets, called "timing CCSDS packets", which are sent via the S-Band real-time down link with the highest priority. The time delay inside the spacecraft from a packet edition in the DP to its acknowledge by the spacecraft transmitter is fixed at 18.0 μs. Since the traveling time from the spacecraft to the ground station depends on the distance between them, the spacecraft location is measured by ranging about twice a day, within an accuracy of 1 km along the line-of-sight, while being about 10 km in three dimensions. Finally, the time delay within the ground station, from the receiver to the recorder, is also known to be less than 2 μs. On each data packet received on ground, "time stamps" are imprinted based on the Rubidium clocks with a 10 or 100 μs timing resolution, depending on which of the 34 m and 20 m antenna systems at USC, respectively, is used to receive the data.

In the second step of the time assignment, TIs issued while the spacecraft is out of contact are converted to UTC values through the TI vs. UTC relation, established in the first step using the closest ground contacts. Since the clock of Suzaku is not placed in a thermostatic environment, its temperature changes with the spacecraft attitude by about ± 20 K around ~ 290 K, leading to temperature-dependent clock drifts. However, this effect was measured on ground, and tabulated before the launch; the table was loaded to the aboard DP. The DP monitors the clock temperature, and calculates every 31.25 ms the corresponding integrated drift time, Y, in units of $1/4096/4096/100\,\mathrm{s} = 0.6\,\mathrm{ns}$. The values of Y are also recorded into the timing CCSDS packets. According to the pre-launch sea-level tests, the TI values after the temperature correction have a stability of about 4×10^{-9}, which accumulates to about 23 μs in one revolution.

2.2. Calculation of Arrival Time of HXD Events

Using the method described in subsection 2.1, we can determine the time values when individual telemetry packets are edited; but what we need to know is the arrival time of each event to the HXD sensor. Considering a mission requirement of a few hundred μs resolution, we designed the HXD so that each event is tagged with its arrival-time information with a resolution of $1/2^{14} = 61.0\,\mu\mathrm{s}$ nominally, and $1/2^{15} = 30.5\,\mu\mathrm{s}$ on condition (selectable by commands). However, because of a severe limitation of the telemetry transfer rate, only 16 bytes information is available per event, which must include not only timing, but also 6 pulse-heights (4 PINs, GSO, and BGO), quality flags, trigger information, and hit-pattern information (Takahashi et al. 1998; Terada et al. 2005). Consequently, only 19 bits per event (hereafter "EventTime") are available for the timing, which covers $1/2^{14} = 61.0\,\mu\mathrm{s}$ to 32 s. Thus, we need to have a mechanism to relate EventTime to the spacecraft time in TI.

Figure 1 shows various timing counters in the HXD electronics, which are also summarized in table 1. The spacecraft clock (subsection 2.1) stays in the data-processing unit (DP), and generates a timing clock of $1/2^{19} = 1.9\,\mu\mathrm{s}$ period. As shown there, the clock is first supplied to HXD-DE, then divided into the control module (Analog Control Unit, ACU) of HXD-AE, and finally supplied into eight analog modules (four Well-type detector Processing Unit, WPU, and four Transient detector Processing Unit, TPU) of HXD-AE.

HXD-DE always holds the latest TI value, supplied from the DP every 2^{19} DP clocks (corresponding to 1 s). In HXD-AE, the time reference is provided by AcuTime in ACU, which is refreshed every 512 s by carry reset signals. The

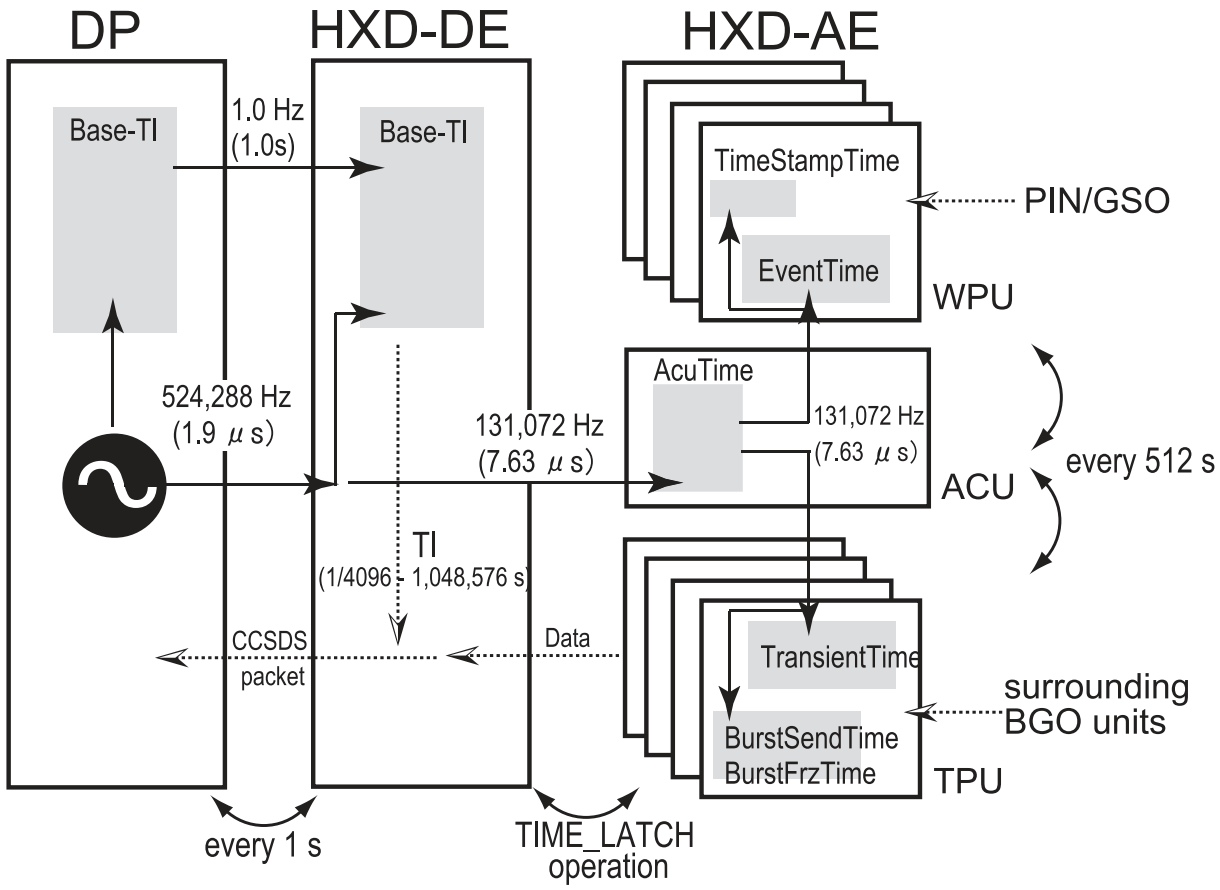

Fig. 1. Timing counters in the HXD electronics.

Table 1. Summary of timing counters of the Hard X-ray Detector.

Name	Component	Length (bit)	Base (s)	Coverage in telemetry (s)	Telemetry type/packet (HK/Event)
Base-TI	DP / Spacecraft	39	$1/2^{19}(1.9\,\mu)$	$1/2^{12}(244\,\mu)$–$2^{20}(1048576)$	HK / time packet
	HXD-DE	39	$1/2^{19}(1.9\,\mu)$	$1/2^{12}(244\,\mu)$–$2^{20}(1048576)$	HK / HXD-HK
AcuTime	HXD-AE ACU	24	$1/2^{17}(7.63\,\mu)$	$1/2^{15}(30.5\,\mu)$–$2^{9}(512)$	HK / HXD-HK
TimeStampTime	HXD-AE WPU	24	$1/2^{15}(30.5\,\mu)$	$1/2^{15}(30.5\,\mu)$–$2^{9}(512)$	HK / HXD-HK
EventTime*	HXD-AE WPU	19	$1/2^{14}(61\,\mu)$	$1/2^{14}(61\,\mu)$–$2^{5}(32)$	Event / HXD_WEL
TransientTime†	HXD-AE TPU	24	$1/2^{15}(30.5\,\mu)$	$1/2^{15}(30.5\,\mu)$–$2^{9}(512)$	Event / HXD_WAM
BurstSendTime	HXD-AE TPU	23	$1/2^{6}(15.6\,\mathrm{m})$	$1/2^{6}(15.6\,\mathrm{m})$–$2^{18}(262144)$	Event / HXD_WAM
BurstFrzTime	HXD-AE TPU	32	$1/2^{15}(30.5\,\mu)$	$1/2^{5}(30.5\,\mathrm{m})$–$2^{18}(262144)$	Event / HXD_WAM

* Time value tagged to each event which detected by a main unit of the HXD sensor.
† Time value used for the HXD-WAM (Wide-band All-sky Monitor: Yamaoka et al. 2006).

values of the counters of AcuTime and TI are synchronized, and cross-checked at the beginning of each observation via TIME_LATCH operation, where they are latched according to the timing chart in figure 2. The latched values of AcuTime and TI are sent to the telemetry, and stored as "HXD_AE_TM_LATCH_TM" and "HXD_TLATCH_TIME" columns in the HXD HK FITS file, respectively. This operation typically occurs once every one to two days. Besides, the eight analog precessing modules in HXD-AE (four WPUs and four TPUs) have such timing counters as "TimeStampTime", "EventTime", "TransientTime", "BurstSendTime", and "BurstFrzTime", which are synchronized to the AcuTime signals.

As explained so far, an X-ray event detected with the HXD is given a UTC time through the following two steps: first, to relate a value of the 19-bit EventTime into the corresponding TI value, and then to convert it into the UTC value, as described in subsection 2.1. In order to conduct the first step without any

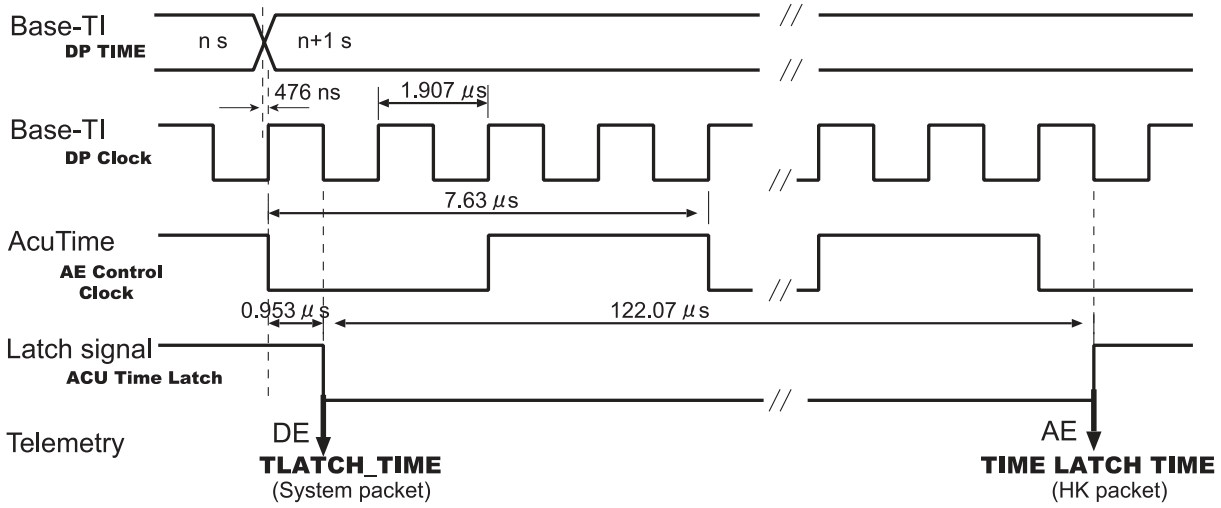

Fig. 2. Timing chart between HXD-AE and HXD-DE at the TIME LATCH operation. DP_TIME and DP_Clock are the signals from DP to HXD-DE to acknowledge time information of the spacecraft, and AE_Control_Clock is provided into HXD-AE from HXD-DE. The signal named ACU_Time_Latch is produced at a time-latch operation in HXD-DE, and is supplied into HXD-AE to verify timings between them.

ambiguity due to scalar overflows, the timing system of the HXD is designed to ensure that the processing and waiting time from the detection of an event to its telemetry output is less than 32 s, which is the coverage of EventTime. The algorithm of the HXD time assignment is implemented in the analysis tool, "hxdtime", in the HEAsoft package.

3. Estimation of Errors in the Time Assignment

3.1. Effects of Spacecraft Location Errors

As described in subsection 2.1, the first step of the time assignment of Suzaku is affected by systematic errors in determinations of the orbital parameters. Due to these errors, the instantaneous spacecraft location has uncertainties of about 10 km, whereas errors along the line-of-sight from the ground station to the satellite are much smaller, about 1 km. Therefore, the air propagation delay of the telemetry can be calculated to an accuracy of 3 μs or so.

In astrophysical analyses of the HXD data, the orbital parameters of Suzaku are also used for another purpose: to perform so-called barycentric corrections, or to convert the arrival times of photons from celestial bodies for light-travel times between Suzaku and the center of gravity of the solar system. We have developed such a tool, named the *aebarycen* in HEAsoft package, to perform the barycentric correction on each event. The correction has three steps: first, using the orbital parameters of the spacecraft, event arrival times are converted to those to be measured at the geodetic center of the Earth; second, to the center of the Sun, and finally to the center of the solar system. The largest conversion in these steps comes from the second one, which is an order of a few hundred seconds (maximum 8 min corresponding to the traveling time from the Sun to the Earth), although it can be calculated accurately from the position of the object and the observation date (i.e., the position of Sun and the Earth). Systematic errors in the overall barycentric correction mainly arise in the first step; the errors of ~ 10 km associated with the satellite position cause the barycentric times to be uncertain by ~ 30 μs.

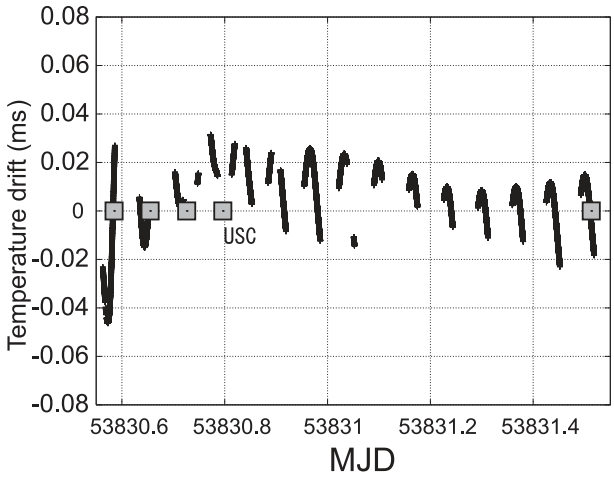

Fig. 3. Example of cumulative clock drifts, expected for the data taken on 2005 September. They are estimated by the measured DP temperature, and the temperature-dependent clock drift rate measured before launch. The horizontal axis shows the Modified Julian Day (MJD). Satellite contacts at the USC are also indicated.

3.2. Effects of Temperature Variation on the Clock

At the second step of the time assignment of data packets (subsection 2.1), namely in the conversion of TIs to UTCs, the clock frequency must be corrected for temperature-dependent drifts. Although the clock stability after the correction was confirmed to be 4×10^{-9} in a pre-flight test (section 1), the relation between the drift rate and DP temperature, used in this correction, was calibrated only on ground, and needs an in-orbit reconfirmation. Before detailed studies described in section 4, figure 3 shows an example of the expected clock drifts to be accumulated; the drift is thus predicted

Table 2. Pulsars observed with Suzaku.

Name	Period	Observation date*	Net exposure of the HXD
Crab	33.58 ms	2005/08–2007/03	200 ks (47 observations)
PSR 1509−58b	151.3533 ms	2005/08/23	44.6 ks
Hercules X-1	1.237 s†	2005/10/05, 2006/03/29	30.7 and 34.4 ks
A 0535+262	103.375 s	2005/09/14	21.3 ks

* In the format of year/month/day.
† Without correcting for the Doppler shifts due to binary motion of the object.

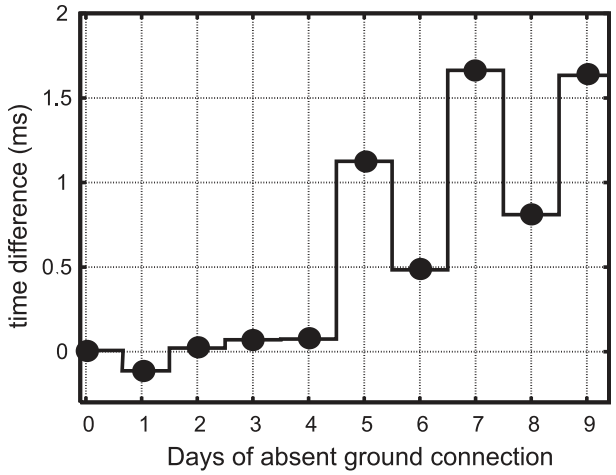

Fig. 4. Time assignment errors introduced to the Crab Nebula data taken on 2003 August 26, when the TI to UTC calibration in the off-line data processing is purposely discarded for various length of time. The horizontal axis shows the duration without ground contacts. The attitude of the satellite was changed on the forth day in the plot to observe another object.

to be typically about 20–40 μs, which introduces systematic errors in the absolute timing by the same order of magnitude in the worst case.

3.3. *Effects of Intervals between Ground Contacts*

The cross-comparison of the TIs to UTC values are performed only at ground contacts. Consequently, systematic errors associated with the time-assignment on packets depend mainly on the time intervals between adjacent contacts. The operations at the down-link station are sometimes canceled due, e.g., to launch campaigns of new satellites, or typhoons attacking the local area. To emulate the effect of the loss of ground contacts, we intentionally, in an off-line data analysis, omitted the TI vs. UTC cross calibrations for a given length of days. Then, as shown in figure 4, the cumulative timing errors increased according to the assumed duration without the ground contacts becoming longer.

4. Results of In-Orbit Timing Calibrations

4.1. *Time Assignment of Random Signals*

As described in subsection 2.2, the data-acquisition system of the HXD is designed to avoid internal data buffering for longer than 32 s. Any failure in the design would produce artifacts in the "time-interval" spectra (occurrence distributions of time difference between adjacent events), which would normally be a simple exponential when the signals are random. We selected in-orbit unfiltered-WEL events (i.e., which include all of PIN, GSO, and BGO events) at various counting rates, and produced time-interval histograms. As shown in figure 5, the derived spectra all exhibit straight lines in semi-log plots, except when the telemetry is saturated. When the HXD event rate becomes so high that the required data flow rate exceeds the telemetry limit, some packets are discarded on HXD-DE every fixed time (1, 2, 4, or 16 s when the data rate of the telemetry is Super High, High, Medium, or Low), and thus, an artificial structure appears in the time-interval spectra; this is seen at 1.7 s in figure 5 for the 480 Hz case.

4.2. *Timing Verification with Periodic Signals*

In the initial performance verification phase of Suzaku, we observed four pulsars listed in table 2. After the barycentric corrections (subsection 3.1), we have successfully detected the periodic signals from them, as shown in periodograms of figure 6. As already reported for several of them (Terada et al. 2006; Enoto et al. 2008), the pulse profiles of these objects observed with the HXD are consistent with those measured in previous observations. The pulsations were also detected in the GSO data of these objects. As shown in figure 7, energy spectra of the pulse component of PSR 1509−58 can be reproduced by a single power-law model up to 300 keV, or higher. The best-fit parameters are a photon index of $1.55^{+0.10}_{-0.09}$ and X-ray flux of $4.86^{+0.34}_{-0.48} \times 10^{-10}$ erg s^{-1} cm^{-2} in the 10–300 keV band. Thus, the HXD has a capability to detect periodic signals in the energy band of 10 to a few hundred keV, from an object of 100 mCrab intensity only in a 45 ks exposure.

4.3. *Relative and Absolute Timing Calibration with Crab*

As listed in table 2, we observed the Crab pulsar 47 times for several calibration purposes including timing, absolute flux, energy spectral shape, and angular response. Among the 47 observations, we selected 23 observations, which had exposures longer than 20 ks, and good statistics to show high power in the period search. As plotted in figure 8 (top), the pulse periods measured on these 23 observations reveal the well-known spin-down trend of the Crab pulsar, which was determined to be $(4.16 \pm 0.02) \times 10^{-13}$ s s^{-1} with our data. This rate agrees with the results by continuous radio-monitoring observations (Lyne et al. 1993).[1] In addition, as shown in figure 8 (bottom), the individual periods obtained by the PIN datasets

[1] See also ⟨http://www.jb.man.ac.uk/~pulsar/crab.html⟩.

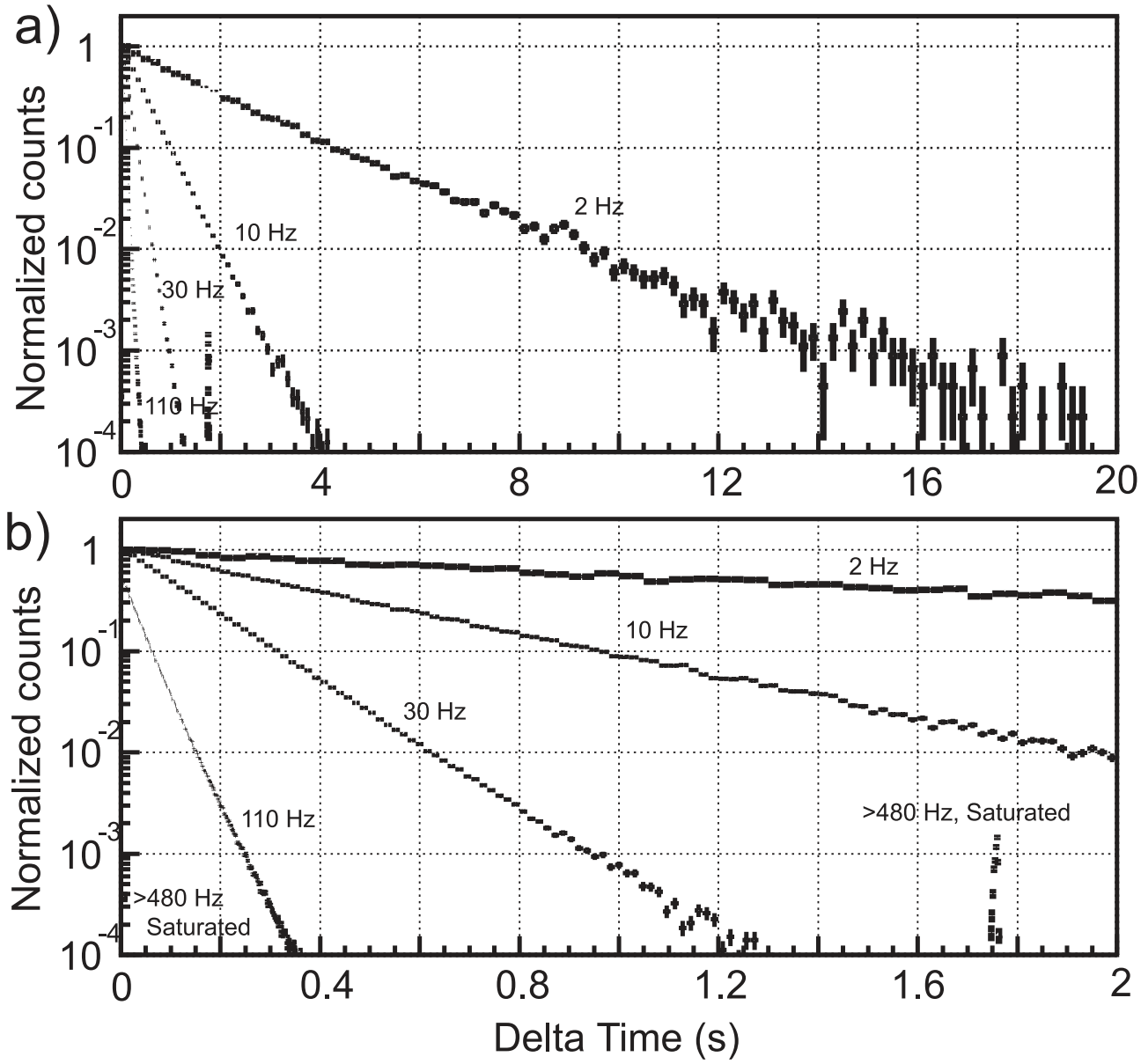

Fig. 5. Examples of time-interval histograms of HXD WEL events at various counting rates, 2, 10, 30, 110, and > 480 Hz. The 2 Hz dataset was derived from cleaned PIN events acquired on 2005 September 14 for 21 ks, and those of 10 and 30 Hz are from GSO events of the Crab observation on 2007 March 20 when the telemetry mode was set for bright sources. Only a quarter of the GSO events were sent to telemetry when the 10 Hz data were acquired. The 110 Hz data set was taken on 2006 May 17 for an exposure of 76 ks (observation of Lockman Hole), and those with > 480 Hz was taken on 2005 September 14 during a daily health-check operation of the PSD function (Takahashi et al. 1998) in which the on-board background rejection was temporally disabled.

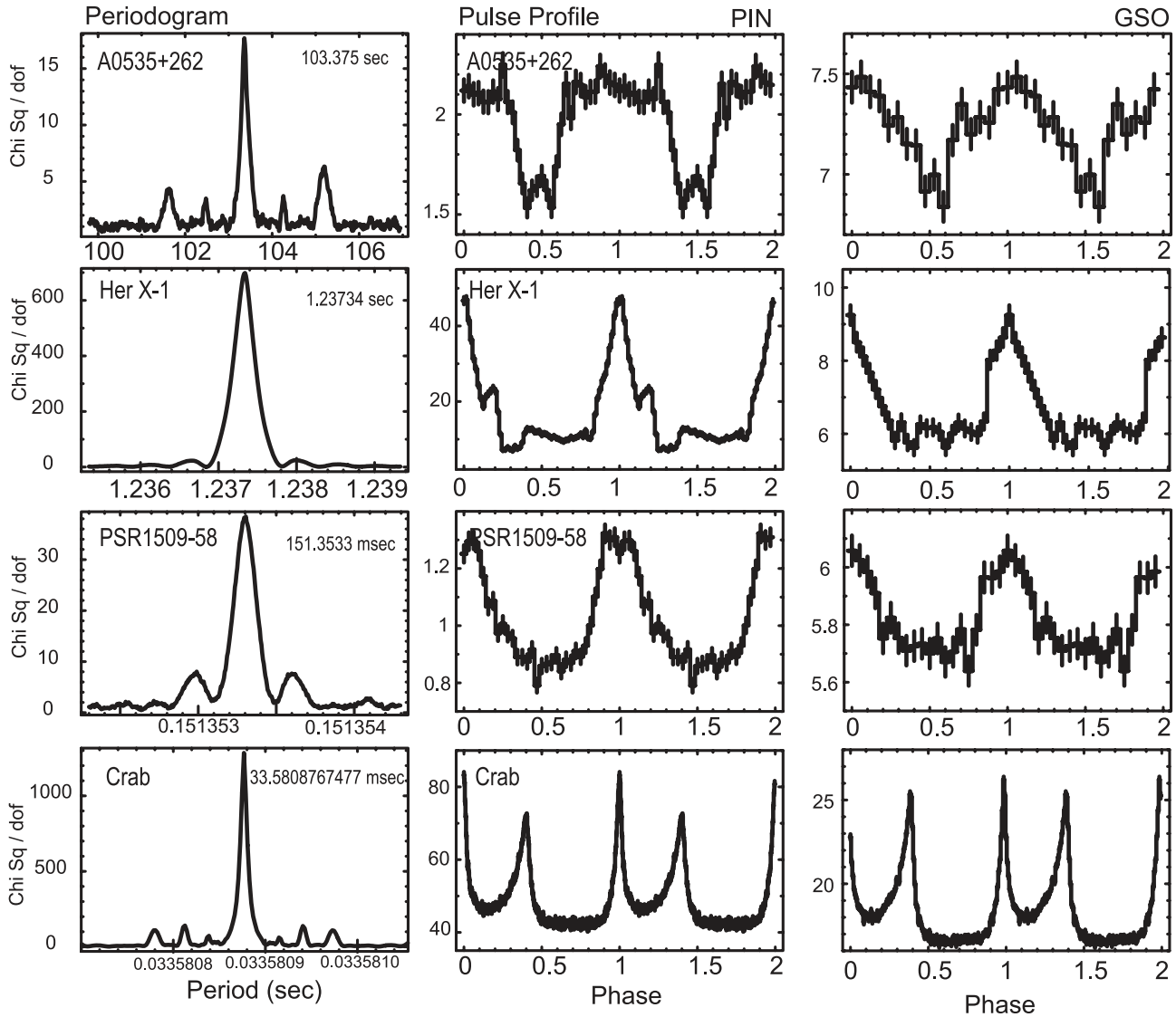

Fig. 6. Periodograms and pulse profiles of A 0535+262, Hercules X-1, PSR 1509−58, and the Crab pulsar, observed with the HXD. Left panels show the periodograms, obtained by PIN in the 10–70 keV band. The vertical axis means a chi-squared value when a light curve, folded at trial periods shown in the horizontal axis, is fitted by a constant. The middle and right panels show pulse profiles by PIN and GSO, respectively, folded at the periods determined by PIN in the left panel.

agree with those measured by the Jodrell Bank Radio observatory (Lyne et al. 1993)[1] within 1.0 ns. The error bars shown here, at 1σ, were determined in reference to Larsson (1996), considering higher harmonics.

The absolute timing of the HXD can be verified by comparing arrival times of the main pulse of Crab with those indicated by the Jodrell Bank Radio ephemeris (Lyne et al. 1993).[1] Thus, on 2007 March 20–21, we performed simultaneous observations of Crab with other X-ray missions, RXTE, INTEGRAL, and Swift. The net exposure of the HXD was 41.1 ks, of which the overlaps with RXTE, INTEGRAL, and Swift were 14.5, 81.3, and 24.8 ks, respectively. The pulse profiles of Crab taken in the campaign are summarized in figure 9. Thus, the X-ray pulses arrive systematically earlier by $\sim$340–500 μs than those in the radio band. This reconfirms a previous report by Rots, Jahoda, and Lyne (2004), who measured the same quantity as 344 μs with RXTE, and discussed possible astrophysical implications. From cross-correlation studies among pulse profiles, the main pulse measured with the Suzaku HXD precedes, by 0.003 ± 0.001, 0.002 ± 0.001, 0.002 ± 0.001, 0.002 ± 0.001 phases, those from the RXTE PCA, the HEXTE, the INTEGRAL IBIS ISGRI, and the Swift BAT, respectively. Thus, in this observation, the absolute timing with the HXD systematically leads by about 160 μs those of the other X-ray instruments.

The time difference between the HXD and the other high-energy experiments in the Crab simultaneous observation is consistent with systematic errors in the HXD timing. We estimate these systematic errors by comparing several HXD-measured arrival phases of the main pulse of Crab, with the Jodrell Bank Ephemeris, as shown in figure 10. The averaged phase of 0.993 is consistent with the other X-ray

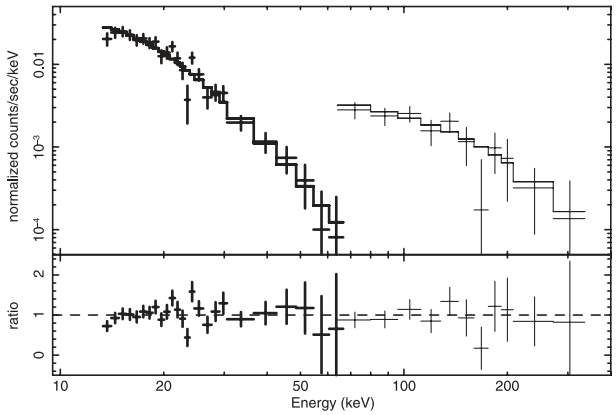

Fig. 7. Pulsed-component spectra of PSR 1509−58, obtained with the HXD by subtracting the pulse-bottom spectra from the one at the pulse peak, reffering to the pulse profile shown in figure 6. The pulse peak and bottom is defined as a pulse phase of 0.0 ± 0.2 and 0.5 ± 0.3, respectively. The data of PIN and GSO are shown by crosses, and the best fit power-law models of them are shown with solid lines. The fitting ranges are 13–70 keV and 70–300 keV band for the PIN and GSO data, respectively.

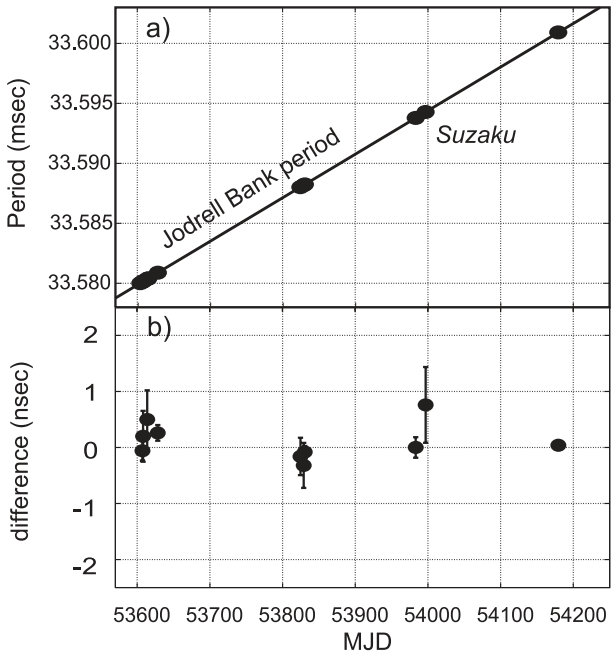

Fig. 8. Pulsation periods of the Crab pulsar obtained by the HXD, compared with the radio measurements (the solid line) at the Jodrell Bank observatory (Lyne et al. 1993). The residuals are shown in the bottom panel. Error bars were determined by the method by Larsson (1996) with a single iteration, and refer to 1σ.

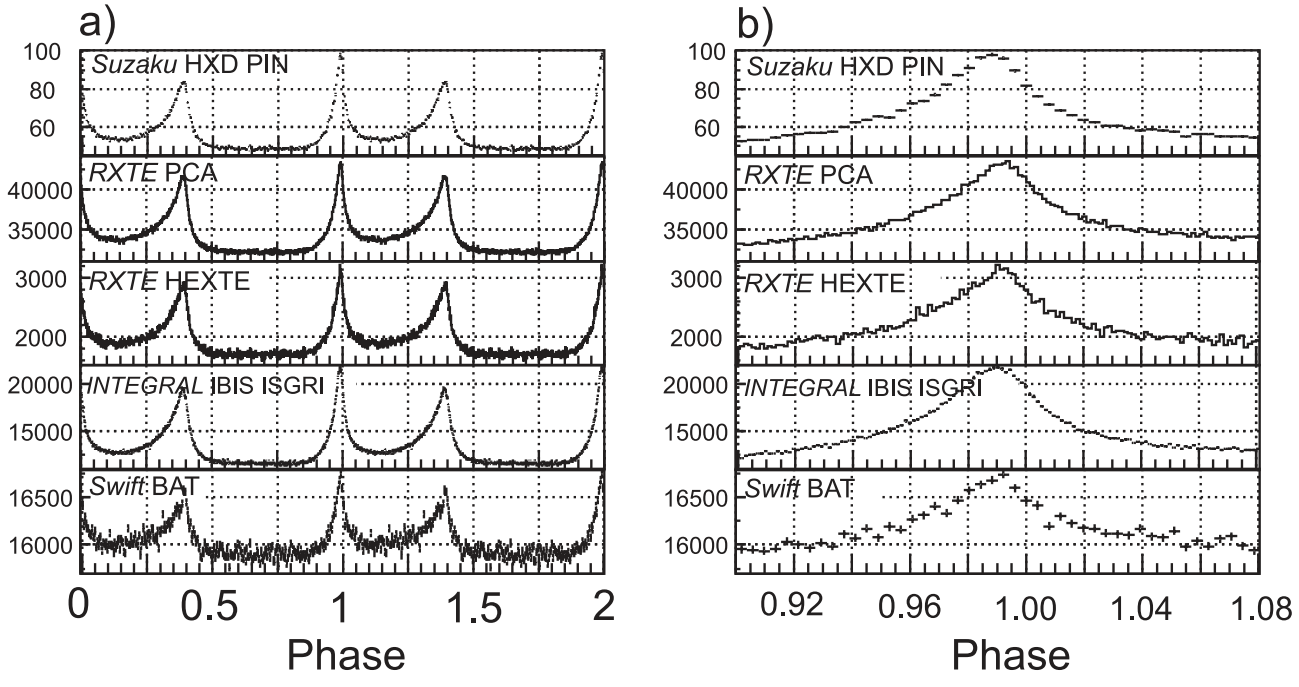

Fig. 9. X-ray pulse profiles of the Crab pulsar obtained by the Suzaku HXD PIN (10–70 keV), the RXTE PCA (2–30 keV), the HEXTE (20–100 keV), the INTEGRAL IBIS ISGRI (20–100 keV), and the Swift BAT (15–350 keV) from top to bottom. The right panel shows the same plot, but expanded to reveal details over the phases of 0.91 to 1.08. The period is 0.03360091293 s, $\dot{P}$ is $4.20506179 \times 10^{-13}$ s s^{-1}, and the phase 0 corresponds to the arrival time of the first pulse obtained by the Jodrell Bank Radio observatory; MJD 54179.4400000438310185391 (where MJD in Terrestrial Time).

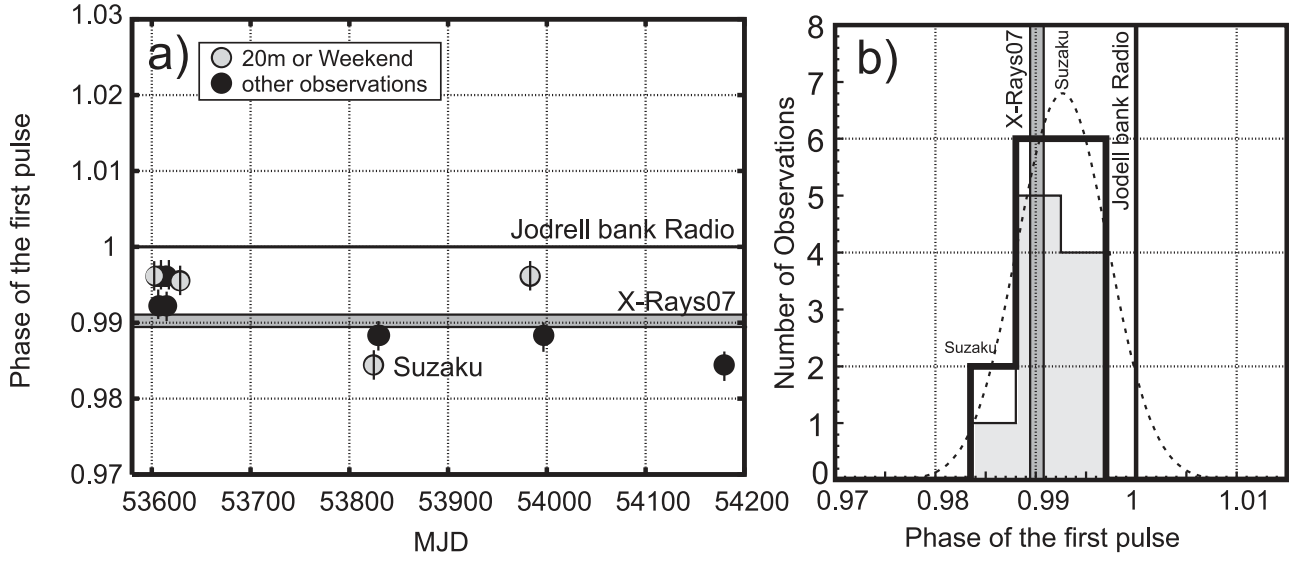

Fig. 10. (Left) Phases of the first pulse of Crab obtained by HXD PIN, compared to the Jodrell Bank ephemeris (Lyne et al. 1993). Phase 0.0 corresponds to the barycentric arrival time of the radio pulses determined by the Jodrell Bank observatory, and the Suzaku data are shown in circles. Open-gray circles show results when the observation was done with the 20 m antenna, or across a lack of ground contacts for > 1 d. The filled circles were taken with the 34 m system on working days. The phases tagged as "X-ray 07" are determined in figure 9 by the X-ray missions in the simultaneous observation on 2007 May. (Right) Distribution (thick histograms) of the 14 phase measurements of the Crab pulse made with the HXD, compared with the radio ephemeris. The shaded histogram shows a distribution of 10 selected observations, which were taken with 34 m antena under daily ground contacts. The dashed curve is a Gaussian fitted to the distribution of all 14 phase measurements.

instruments used for the simultaneous observations. Since the phases measured with the HXD thus scatter by about 0.010 ± 0.005 phases (with 90% error), the total systematic error in the absolute timing of the HXD is concluded to be about $360 \pm 150\,\mu$s. If we discard datasets taken with the 20 m antenna system, or those obtained across a lack of ground contacts for > 1 d, the dispersion reduces to $270 \pm 130\,\mu$s. Although the particular case of figure 9 revealed a systematic offset (by $\sim 160\,\mu$s) of the HXD timing from those of other instruments, this is within the estimated systematic error of $\sim 270\,\mu$s. On the other hand, the phases of the main pulses stay within 0.005 phases within an observation, implying that the stability of the arrival time measurements is within 1.9×10^{-9}.

5. Conclusion

Systematic errors on the HXD timing due to spacecraft location errors, the temperature-dependence of the on-board clock, and between ground contacts (if the altitude is not changed), are ~ 30, < 40, and $< 150\,\mu$s, respectively. Using the Crab pulsar, we confirmed the stability of the relative timing to be 1.9×10^{-9} s s^{-1} per day. The systematic errors on the HXD absolute time have been calibrated as about $360\,\mu$s or higher ($\sim 270\,\mu$s under daily ground contacts with the 30 m antenna system).

We would like to thank all members of the Suzaku Science Working Group, for their contributions to the instrument preparation, spacecraft operation, software development, and in-orbit instrumental calibration. We also deeply thank Dr. Richard Rothschild, Dr. Keith Jahoda, Dr. Arnold H. Rots, Dr. Christoph Winkler, Dr. Wim Hermsen, Dr. Erik Kuulkers, Dr. Jean Swank, Dr. Goro Sato, Dr. Takanori Sakamoto, and the operation teams of RXTE, INTEGRAL, and Swift, for their efforts on the simultaneous observation of Crab and quick analyses of the data.

References

Enoto, T., et al. 2008, PASJ, 60, S57
Kawaharada, M., et al. 2004, Proc. SPIE, 5501, 286
Kokubun, M., et al. 2004, IEEE Trans. Nucl. Sci., 51, 1991
Kokubun, M., et al. 2007, PASJ, 59, S53
Larsson, S. 1996, A&AS, 117, 197
Lyne, A. G., Pritchard, R. S., & Graham Smith, F. 1993, MNRAS, 265, 1003
Mitsuda, K., et al. 2007, PASJ, 59, S1
Ohno, M., et al. 2005, IEEE Trans. Nucl. Sci., 52, 2758
Rots, A. H., Jahoda, K., & Lyne, A. G. 2004, ApJ, 605, L129
Sugiho, M., et al. 2001, IEEE Trans. Nucl. Sci., 48, 426
Takahashi, T., et al. 1998, Proc. SPIE, 3445, 155
Takahashi, T., et al. 2007, PASJ, 59, S35
Tashiro, M., et al. 2002, IEEE Trans. Nucl. Sci., 49, 1893
Terada, Y., et al. 2005, IEEE Trans. Nucl. Sci., 52, 902
Terada, Y., et al. 2006, ApJ, 648, L139
Uchiyama, Y., et al. 2001, IEEE Trans. Nucl. Sci., 48, 379
Yamaoka, K., et al. 2006, IEEE Trans. Nucl. Sci., 52, 2765